Differences Between Thermal and Laser-Induced Diffusion

Ch. Zaum,[1] K. M. Meyer-auf-der-Heide,[1] M. Mehlhorn,[1] S. McDonough,[2] W. F. Schneider,[2] and K. Morgenstern[3,*]

[1]*Leibniz Universität Hannover, Institut für Festkörperphysik, Abteilung für atomare und molekulare Strukturen (ATMOS),
Appelstrasse 2, D-30167 Hannover, Germany*
[2]*Departement of Chemical and Biomolecular Engineering, University of Notre Dame, Notre Dame, Indiana 46556, USA*
[3]*Ruhr-Universität Bochum, Lehrstuhl für physikalische Chemie I, D-44780 Bochum, Germany*

A combination of femtosecond laser excitation with a low-temperature scanning tunneling microscope is used to study long-range interaction during diffusion of CO on Cu(111). Both thermal and laser-driven diffusion show an oscillatory energy dependence on the distance to neighboring molecules. Surprisingly, the phase is inverted; i.e., at distances at which thermal diffusion is most difficult, it is easiest for laser-driven diffusion and vice versa. We explain this unexpected behavior by a transient stabilization of the negative ion during diffusion as corroborated by *ab initio* calculations.

The fundamental investigation of chemical reactions at surfaces aims at an increase of the reaction yield, which is important to areas as diverse as heterogeneous catalysis, electrochemistry, and nanoscale technology. Reactions are usually driven directly by heat, i.e., phonon mediated, or indirectly by radiation adsorbed in the support, i.e., electron mediated. In the latter case, the reaction is called non-adiabatic, because the first initial excitation step involves a fast transfer of an electron from a ground to an excited state. In consequence, electron and phonon systems are not in equilibrium. In the former, adiabatic case, both the electron and phonon system are at the same temperature. Often, both types of adsorbate heating contribute to the reaction yield.

Diffusion is a component of every surface reaction. Thus, thermally driven adsorbate diffusion on surfaces has been studied intensively [1]. Studies of laser-induced adsorbate diffusion are rarer [2,3], and only a very few local investigations exist at the single molecule level [4–6]. Two studies pinpointed qualitative differences between thermal and laser-driven diffusion, but the reason for these differences remains to be revealed [5,6].

Most surface diffusion studies are performed at dilute coverage [1]. For high adsorbate coverage, adsorbate interactions have to be considered. On metallic fcc(111) surfaces, an oscillatory adsorbate interaction is mediated by electrons in the surface state [7]. This interaction leads to a modification of the diffusion potential Φ on nanometer distances [8,9]. The interaction energy is given by the asymptotic interaction term $\Delta E_{\text{pair}}(d)$ [8]:

$$\Delta E_{\text{pair}}(d) = -A(r,\varphi)\frac{4}{\pi^2}\epsilon_F\frac{\sin(2k_F d + 2\varphi)}{(k_F d)^2} \quad (1)$$

for two interacting adsorbates with distance d and well separated from all other adsorbates.

Here, ϵ_F, k_F, and φ are the onset energy, the Fermi wave vector, and the scattering phase of the surface state electrons, respectively. For a perfect scatterer with reflectivity $r = 1$ and phase shift $\varphi \approx \pi/2$, the complex prefactor simplifies to $A = \sin^2\varphi$. The interaction energy decreases with increasing adsorbate separation and oscillates at half of the Fermi wavelength of the surface state.

In this Letter, we investigate the impact of long-range interaction on the diffusion of CO molecules on Cu(111) for both thermally driven and laser-induced motion by scanning tunneling microscopy and compare their oscillatory distance dependence. We reveal a surprising phase shift of the oscillating interaction for the two excitation sources. We rationalize this unexpected difference by a stabilization of charge on the diffusing molecule.

The experiments were performed with a custom-built instrument that combines atomic resolution of a low-temperature UHV-STM with the ultrafast surface dynamics driven by femtosecond laser excitation [10]. Cu(111) is cleaned by standard sputtering and annealing cycles. Then, 0.01 or 0.02 ML of CO is deposited at 22 K via a leak valve. Diffusion of the molecules is induced either by *in situ* heating for measurements between 30 and 38 K or via femtosecond laser excitation [6]. Special care is taken to reduce the drift during the measurement to negligible values and to carefully stabilize and exactly determine the temperature at the sample by calibrating the temperature diodes used to high precision and by determining the temperature drop between the position of the Si diode and the sample [11].

For the laser excitation, the sample is cooled to 7 K to suppress any thermal motion. The frequency doubled laser pulses of a Ti:sapphire oscillator have a duration of 40 fs at 400 nm (3.1 eV photon energy) and a repetition rate of 10 MHz. At an absorbed fluence of ≈ 5 J/m^2, 5×10^8 pulses are given with the tip retracted to avoid far- and near-field tip effects during the irradiation [11].

In our calculation, we used a supercell slab model and density functional theory (DFT) to compare the site preferences and diffusion potentials seen by charged and neutral CO on Cu(111) [11].

CO diffusion is followed in consecutive images taken either at elevated temperature or before and after laser illumination. Figures 1(a)–1(e) show such a series of STM images recorded at 32.5 K at the same spot of the surface at regular time intervals. Each CO molecule is imaged as a ~30 pm deep depression. The electrons that mediate the long-range interaction are visible on such images as circular standing waves around the molecules.

The molecules change position between the images. In total, 3400 images representing 190 h of diffusion of 2200 CO molecules are recorded within several image sequences. In each sequence, the center of mass of every CO molecule is determined via a 2D Gaussian fit and followed in time [11]. Positions within the movie of the six CO molecules marked in Figs. 1(a)–1(e) are shown in Fig. 1(f). The CO molecules diffuse randomly on a hexagonal lattice. This lattice corresponds to the atop sites of Cu(111) [11]. After having ensured that the motion is a random motion,
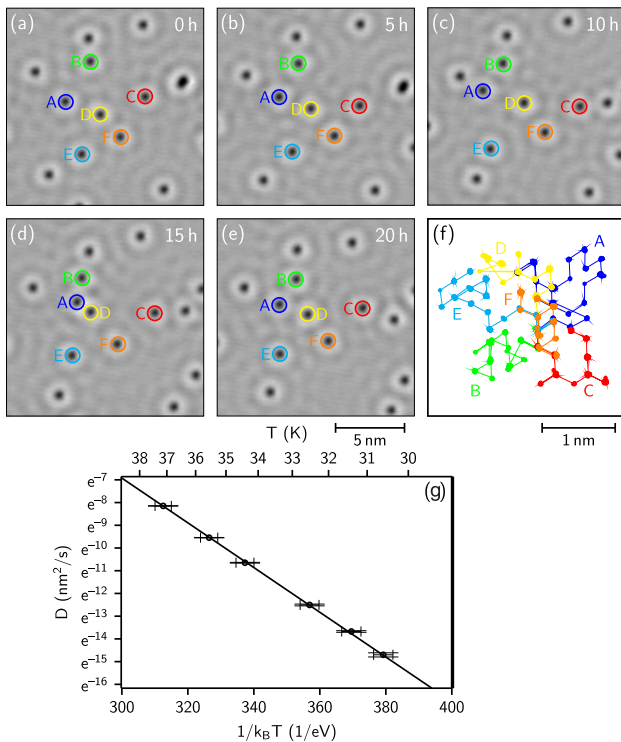

FIG. 1 (color online).   Thermal diffusion: (a)–(e) Snapshots of the image sequence at the indicated time (400 images, 180 s/image, $I = 44$ pA, $V = 200$ mV, and $T = 32.5$ K). (f) Relative positions of CO molecules circled in (a)–(e) for all images of the movie; for an impression of the motion, see the movies [11]. (g) Arrhenius plot based on ≈ 300.000 molecule positions: the black line is linear fit; y-error bars are displayed with a small linewidth and extended cap length to make them visible.

we extract the diffusivity D via the Einstein relation $\langle \Delta x^2 \rangle = 2D\Delta t$ in dependence of temperature.

We start by determining the average diffusion barrier E_D from the measured diffusivity D regardless of the neighbor's positions via the Arrhenius temperature dependence: $D = D_0 e^{-E_D/kT}$ with T the temperature and k the Boltzmann constant. The Arrhenius plot yields $E_D = (98.4 \pm 0.5)$ meV and $D_0 = 6.5 \times 10^{9.0 \pm 0.1}$ nm²/s [Fig. 1(g)]. The diffusion barrier compares well to the value of $E_D = (98 \pm 5)$ meV determined recently in helium-spin-echo measurements [12]. It is larger than the one determined earlier for laser-induced diffusion of $E_D = (87 \pm 3)$ meV at a prefactor of $10^{12.6 \pm 0.3}$ Hz [6]. This quantitative difference between the differently excited diffusive motions is surprising. Nonadiabatic diffusion barriers are generally expected to be around 30% *larger* than the corresponding barriers for thermally activated diffusion, because not only diffusion paths at the lowest activation energy are followed by the nonadiabatically excited molecule [2,13]. Moreover, a different prefactor is not expected for motion on the same surface. As the prefactor reflects the difference in entropy between the ground and transition state, it implies that the motion is qualitatively different in the two cases.

The influence of neighboring molecules on the diffusion is analyzed by determining the distance d of each molecule to its nearest neighbor (NN) and subsequently the diffusion constant for different NN distances via the Einstein relation. From Arrhenius graphs, we determine a distance-dependent diffusion barrier E_D [Fig. 2(a)] [11]. Indeed, the interaction energy oscillates. Fitting $\Delta E_D = \alpha \Delta E_{\mathrm{pair}}$ [see Eq. (1)] with α an empirical fitting parameter yields $k_F = (2.1 \pm 0.1)$ nm^{-1}, $\varphi = (0.6 \pm 0.1)\pi$, and $\alpha = 0.03 \pm 0.01$. The value for k_F is in excellent agreement with the Fermi wave vector of the Cu(111) surface state electrons of $k_F = \sqrt{2m^* \epsilon_F}/\hbar = 2.1$ nm^{-1} [14], and the diffusion barrier oscillates at half of the Fermi wavelength. In contrast, the amplitude is only 3% of the expected value.

Such a deviation has been observed before [15,16] but not convincingly explained yet. Based on simulations presented in Figs. 2(b)–2(d), we are able to explain the fact that the measured energy barrier oscillates much less than theoretically predicted. In the simulations, we mimic the diffusion potential probed by the molecule by mapping the potential derived from the theoretically predicted oscillatory pair interaction energy E_{pair} [Eq. (1)] at the material values for Cu(111) onto the two-dimensional hexagonal diffusion lattice at $a_{\mathrm{Cu(111)}} = 255.6$ pm and derived from the above determined diffusion barrier $E_D = 98.4$ meV. We thus achieve the total potential shown in Figs. 2(b) and 2(d). The distance-dependent change of the barrier ΔE shows a deviation from the average diffusion barrier of up to 35 meV [Fig. 2(c), dashed line]. Next, we mimic the experimental measurement by averaging ΔE over similar distance intervals as in the experiment

FIG. 3. Phase: Difference $\Delta\varphi = \varphi^0 - \varphi_{\rm fit}$ between scattering phase φ^0 assumed in the calculation and the scattering phase $\varphi_{\rm fit}$ obtained from fits as in Fig. 2(c); the solid line is the empirical cosine fit.
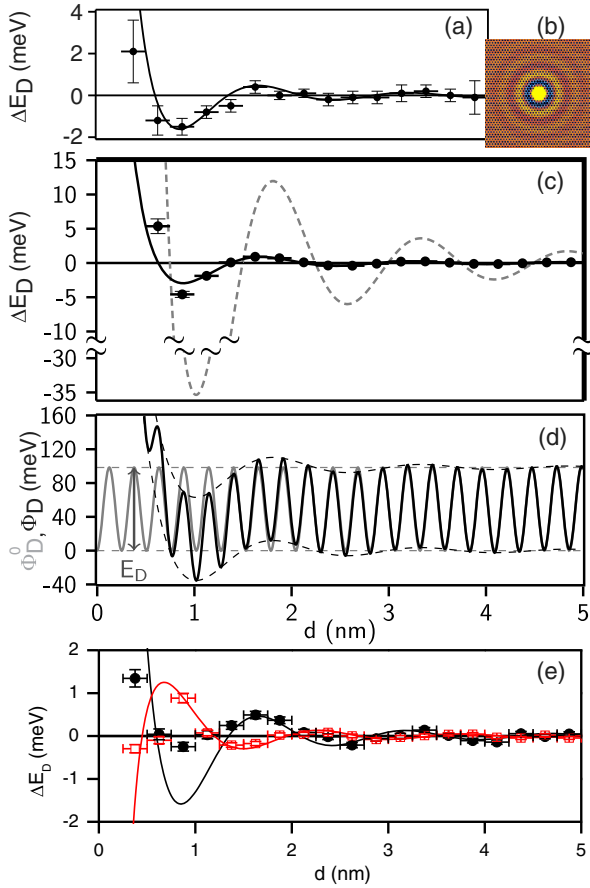
FIG. 2 (color online). Distance-dependent diffusion; solid lines are fits as described in the text: (a) Difference ΔE_D to mean value for thermal diffusion determined in a tracer diffusion experiment. (b) Two-dimensional potential constructed by superposition of the potential based on the energy barrier determined from Fig. 1(g) and the oscillating energy from Eq. (1), 10 nm × 10 nm. (c) Difference ΔE_D deduced from averaging E_D [see (d)] over distance intervals of 0.25 nm, as indicated by bars, compared to the originally assumed pair interaction energy (dashed gray line). (d) Calculated diffusion potential without considering (gray line) and with considering (black line) pair interaction. (e) ΔE_D for diffusion determined from distance distributions: solid circles are for thermal diffusion at $T = 33.2$ K; open squares are for laser-induced CO diffusion at 5 J/m^2.

[Fig. 2(c), dots]. The calculated values have an amplitude of 5 meV at most, considerably less than the input amplitude of 35 mV. Fitting the pair interaction energy yields the same Fermi wave vector but $\alpha = 0.064 \pm 0.003$. The amplitude ratio is thus comparable to the one in the experiment.

The phase extracted from the fit to the calculated potential is, at $\varphi_{\rm fit} = (0.58 \pm 0.02)\pi$, larger than the assumed scattering phase (input value in the calculation) of $\varphi^0 = \pi/2$. This deviation implies that also the phase measured in the experiment deviates from the real scattering phase. We thus used different input values φ^0
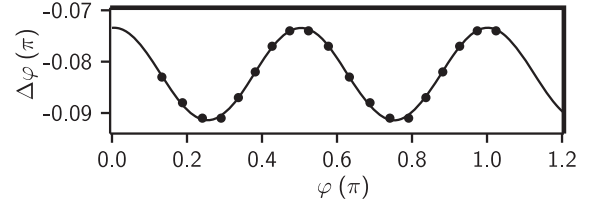
in our calculation and determined the phase difference $\Delta\varphi = \varphi^0 - \varphi_{\rm fit}$ between the input value φ^0 and the phase $\varphi_{\rm fit}$ as determined by fitting to the calculated potential after averaging [similar to Fig. 2(c)]. The difference $\Delta\varphi$ is plotted in Fig. 3. It oscillates between -0.07π and -0.09π and is empirically fitted by a sinusoidal curve. Based on this result, we calculate the real scattering phase of the surface state electrons at a CO molecule during thermal diffusion via $\varphi + \Delta\varphi$ to be $\varphi^{\rm therm} = (0.5 \pm 0.1)\pi$. This value corresponds to the value expected for a perfect scatterer [15].

Though our setup allows us following the laser-driven motion of individual molecules [6], the image acquisition rate of less than one image per hour inhibits a similar large statistics. Instead, we explore distance histograms as in previous studies of long-range effects during thermal diffusion [15,16]. In these studies, the distance-dependent change in diffusion energy ΔE is determined by measuring all distances d_{ij} between all pairs of CO molecules on a STM image. In a histogram at bin size Δd the probability is $P_0(d) = N_0(d)C(d)$ for a random distribution of noninteracting adsorbates [15], with $N_0(d) = 2\pi d \Delta d n^2/L^2$ the distribution for infinite image size, n the number of adsorbates, and a correction factor $C(d) = 1 - d(4L - 4d + \pi d)/\pi L^2$ for finite image size L.

Figure 4 compares distance distributions for thermal CO diffusion to those for laser-induced CO diffusion. The measured data for both the adiabatic diffusion [Figs. 4(a) and 4(c)] and the nonadiabatic one [Figs. 4(b) and 4(d)] oscillate at a similar period; i.e., both interactions are mediated by the surface state electrons. However, the phase differs [compare Fig. 4(c) to 4(d)].

To investigate this phase difference further, we calculate the interaction energy ΔE from the histogram. For thermal diffusion, the distance-dependent change in interaction energy at diffusion temperature T is extracted from the deviation of the measured histogram P from the interaction-free histogram P_0 [15]:

$$\Delta E = -kT \ln(P/P_0). \qquad (2)$$

Fitting the thermal diffusion by $\Delta E_D^{\rm therm} = \alpha \Delta E_{\rm pair}$ yields $k_F^{\rm therm} = (2.1 \pm 0.1)$ nm^{-1}, $\varphi^{\rm therm} = (0.60 \pm 0.07)\pi$,
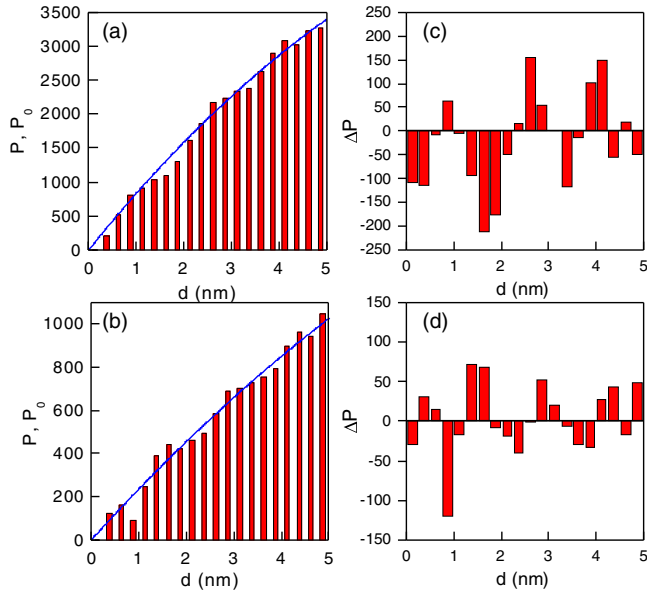
FIG. 4 (color online). Comparison of thermal to laser-driven diffusion at $\rho_{CO} = 0.02$ ML: (a),(b) Distance distributions as measured P (bars) and as expected for interaction-free motion P_0 on finite image size (solid line) and (c),(d) difference $\Delta P = P_0 - P$ for (a),(c) thermal CO diffusion at $T = 33.2$ K and (b),(d) laser-induced CO diffusion at 5 J/m^2 [17].

and $\alpha^{therm} = 0.04 \pm 0.01$ [Fig. 2(e)]. These parameters are in excellent agreement with the values determined in the tracer diffusion experiment.

Calculation of the interaction energy from the laser-induced distance distribution is less straightforward, because the adsorbate temperature varies during laser excitation [18]. As this temperature variation does not depend on the adsorbate-adsorbate distance, we empirically use an "effective" temperature T_{eff} in Eq. (2). This is sufficient for our purpose of determining the phase. We fit $\Delta E_D^{fs} = \alpha^{therm} \Delta E_{pair}$ to the thus obtained data in Fig. 2(e) by utilizing the prefactor determined for thermal diffusion above, because the deviation as explained above should be identical in the two experiments. The fit yields $T_{eff} = 12$ K, $k_F^{fs} = (2.1 \pm 0.1)$ nm^{-1}, and $\varphi^{fs} = (0.1 \pm 0.1)\pi$. The Fermi wave vectors are identical within the error bars, but the phase differs by $\approx \pi/2$.

A different phase points to different scattering properties of the CO molecules. But how can the excitation source alter the scattering properties of a molecule? We recall that a major difference between the two excitation sources is the abundance of hot electrons, i.e., charged particles, in the laser-driven case. The charge dependence of scattering properties of a particle is given by Friedel's sum rule. For the s-like waves in the surface state, this rule states that $q = 2e/\pi\varphi$. Based on this relation, we calculate a charge difference $\Delta q = |q_{fs} - q_{therm}| = 2e/\pi\Delta\varphi$ of the diffusing molecules in the two experiments from the measured phase difference $\Delta\varphi = |\varphi_{fs} - \varphi_{therm}|$. Equation (1) determines

the phase only modulo π resulting in two possible phase differences $\Delta\varphi_a = |(\varphi_{fs} \pm n\pi) - (\varphi_{therm} \pm n\pi)| = (0.4 \pm 0.1)\pi$ or $\Delta\varphi_b = |(\varphi_{fs} \pm n\pi) - (\varphi_{therm} \mp n\pi)| = (0.6 \pm 0.1)\pi$ corresponding to charge differences of $\Delta q_a = (0.8 \pm 0.2)e$ or $\Delta q_b = (1.2 \pm 0.2)e$, i.e., approximately one electron. The well-resolved distance dependence suggests that we are observing the diffusion of the charged molecule rather than of uncharged molecules traveling in a dilute mixture of charged and uncharged adsorbates in laser-driven diffusion.

Thermal diffusion is well established to proceed in the electronic ground state. The gas-phase ground state electronic configuration of CO is $(1\pi)^4(5\sigma)^2$. The observed $\approx 1e$ charge difference during laser-induced diffusion is achieved by occupation of the first negative ion resonance CO$^-(2\pi^*)$ of the CO molecule. Note that the laser pulses excite substrate electrons, not the adsorbed CO molecules [19]. These excited electrons transiently occupy the CO $2\pi^*$ state and transfer part of their energy to molecular vibrations [20]. Anharmonic coupling of the excited internal vibrations to the frustrated translation and/or frustrated rotation then leads to diffusion [6,21]. However, the diffusion itself was assumed to occur in the electronic ground state [22].

The time scales involved in this generally accepted model are inconsistent with the present experimental observations. We measured distance distributions well after the laser-induced diffusion was complete and the system returned to the thermal equilibrium. If CO diffusion continued after the electronically excited state had decayed, its scattering phase would change and the distance distribution could not retain the phase. This implies that the charge difference has to be present during the latter part of the diffusion. However, the mean lifetime of an electron in the $2\pi^*$ orbital of a CO molecule adsorbed in the atop site on Cu(111) is less than 5 fs [20,23], much shorter than the time scale of its laser-induced diffusion of up to 300 fs [24]. We point out that already the vibrational excitation that is necessary to induce either desorption [20] or diffusion [6] demands a lifetime of the electron on the molecule that is longer than its mean lifetime. This prerequisite might be at the origin of the very low efficiencies of both processes.

The evidence presented above points to a scenario in which CO retains excess charge during diffusion, perhaps associated with migration to a different adsorption site. We used supercell DFT calculations to contrast uncharged and charged Cu-bound CO. As shown in Fig. 5 and described in Supplemental Material [11], uncharged CO prefers adsorption atop Cu [25], carries a dipole that points into the surface, and has vacant $2\pi^*$ states above the Fermi level. Neutral CO experiences repulsive dipolar interactions with like neighbors. When charge is injected into the system, the CO preference shifts to a threefold site, where it sits nearer the surface and carries a net negative charge. The relative energies of all sites are more similar in the charged than
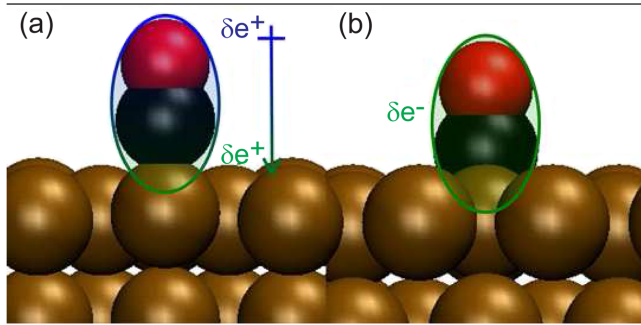
FIG. 5 (color online). Generalized gradient approximation computed structures and charge distributions of CO on Cu(111) in the (a) absence and (b) presence of an excess electron leading to the (a) uncharged CO atop site and (b) charged CO-fcc bond.

uncharged case, so that the charged CO probes a different and shallower potential energy surface, consistent with the 10 meV lower diffusion barrier for laser-driven diffusion. Such a qualitatively different diffusion scenario is corroborated by the difference in prefactor, i.e., entropy (see above).

After its discharge the neutral molecule changes back to an atop site. Though being possibly still vibrationally excited, the sudden increase in diffusion barrier will impede further diffusion of an originally charged molecule. Thus, the distance distribution established during the diffusion in its charged state is maintained [26].

In conclusion, we demonstrate important differences between thermal and laser-driven diffusion. Not only the energy barrier and the prefactor differ, but also the moving particle in laser-induced diffusion is charged and by this moves on another surface potential than the thermally diffusing particle. So far proposed diffusion mechanisms for laser-induced diffusion have thus to be reconsidered regardless of whether long-range interactions are involved or not.

---

*karina.morgenstern@rub.de

[1] G. Antczak and G. Ehrlich, *Surface Diffusion* (Cambridge University Press, Cambridge, England, 2010).

[2] K. Stépán, J. Güdde, and U. Höfer, Phys. Rev. Lett. **94**, 236103 (2005).

[3] E. H. G. Backus, A. Eichler, A. W. Kleyn, and M. Bonn, Science **310**, 1790 (2005).

[4] M. Mehlhorn, J. Carrasco, A. Michaelides, and K. Morgenstern, Phys. Rev. Lett. **103**, 026101 (2009).

[5] L. Bartels, F. Wang, D. Möller, and T. F. Heinz, Science **305**, 648 (2004).

[6] M. Mehlhorn, H. Gawronski, and K. Morgenstern, Phys. Rev. Lett. **104**, 076101 (2010).

[7] P. Han and P. S. Weiss, Surf. Sci. Rep. **67**, 19 (2012).

[8] P. Hyldgaard and M. Persson, J. Phys. Condens. Matter **12**, L13 (2000).

[9] P. Hyldgaard and T. L. Einstein, Europhys. Lett. **59**, 265 (2002).

[10] M. Mehlhorn, H. Gawronski, L. Nedelmann, A. Grujic, and K. Morgenstern, Rev. Sci. Instrum. **78**, 033905 (2007).

[11] See Supplemental Material at http://link.aps.org/supplemental/10.1103/PhysRevLett.114.146104 for temperature and lattice calibration, data analysis, and computational methods.

[12] P. R. Kole, H. Hedgeland, A. P Jardine, W. Allison, J. Ellis, and G. Alexandrowicz, J. Phys. Condens. Matter **24**, 104016 (2012).

[13] A. C. Luntz, M. Persson, S. Wagner, C. Frischkorn, and M. Wolf, J. Chem. Phys. **124**, 244702 (2006).

[14] M. F. Crommie, C. P. Lutz, and D. M. Eigler, Nature (London) **363**, 524 (1993).

[15] J. Repp, F. Moresco, G. Meyer, K. H. Rieder, P. Hyldgaard, and M. Persson, Phys. Rev. Lett. **85**, 2981 (2000).

[16] F. Silly, M. Pivetta, M. Ternes, F. Patthey, J. Pelz, and W.-D. Schneider, Phys. Rev. Lett. **92**, 016101 (2004); M. Ternes, C. Weber, M. Pivetta, F. Patthey, J. Pelz, T. Giamarchi, F. Mila, and W.-D. Schneider, Phys. Rev. Lett. **93**, 146805 (2004); T.-Y. Fu, Y.-J. Hwang, and T. T. Tsong, Surf. Sci. **566**, 462 (2004); H. Y. Lin, Y. Chiu, L. Huang, Y. Chen, T. Fu, C. Chang, and T. Tsong, Phys. Rev. Lett. **94**, 136101 (2005); N. N. Negulyaev, V. Stepanyuk, L. Niebergall, P. Bruno, M. Pivetta, M. Ternes, F. Patthey, and W.-D. Schneider, Phys. Rev. Lett. **102**, 246102 (2009).

[17] Though within the confidential interval given by the error bars, the larger deviation of the experimental values at around 1 nm distance from the mean best fit might result from trio interactions that were theoretically predicted: T. Einstein, Surf. Sci. **84**, L497 (1979). Some experimental evidence for such a trio interaction for CO on Cu(111) exists: C. Zaum, Ph.D. thesis, University of Hannover, 2013.

[18] C. Frischkorn and M. Wolf, Chem. Rev. **106**, 4207 (2006).

[19] J. C. Tremblay, S. Beyvers, and P. Saalfrank, J. Chem. Phys. **128**, 194709 (2008); J. C. Tremblay, G. Füchsel, and P. Saalfrank, Phys. Rev. B **86**, 045438 (2012).

[20] L. Bartels, G. Meyer, K.-H. Rieder, D. Velic, E. Knoesel, A. Hotzel, M. Wolf, and G. Ertl, Phys. Rev. Lett. **80**, 2004 (1998).

[21] H. Ueba, Y. Ootsuka, M. Paulsson, and B. N. J. Persson, Phys. Rev. B **82**, 121411(R) (2010).

[22] H. Ueba, Surf. Sci. **601**, 5212 (2007).

[23] J. P. Gauyacq, A. G. Borisov, and G. Raseev, Surf. Sci. **490**, 99 (2001).

[24] J. A. Prybyla, H. W. K. Tom, and G. D. Aumiller, Phys. Rev. Lett. **68**, 503 (1992).

[25] E. J. Moler, S. A. Kellar, W. R. A. Huff, Z. Hussain, Y. Chen, and D. A. Shirley, Phys. Rev. B **54**, 10862 (1996); L. Bartels, G. Meyer, and K.-H. Rieder, Surf. Sci. Lett. **432**, L621 (1999).

[26] Though the lateral shift due to the change in adsorption site would lead to a slight change in distance, this is an order of magnitude smaller than the observed phase shift.